Efficient Modeling of Dynamic Blockage Effects for Unsteady Wind Tunnel Testing

Sumant Sharma
ssharma46@gatech.edu
Undergraduate Research Assistant

Vrishank Raghav
vrishank@gatech.edu
Graduate Research Assistant

Narayanan Komerath*
komerath@gatech.edu
Professor

Marilyn Smith
marilyn.smith@ae.gatech.edu
Professor

Daniel Guggenheim School of Aerospace Engineering
Georgia Institute of Technology
Atlanta, GA, USA

ABSTRACT

Elementary solutions of the Laplace equation for incompressible flow are used to explore the influence of wind tunnel walls on the growth of instabilities of a tethered bluff body. The tethered body is modeled as a compound pendulum in a plane orthogonal to a steady freestream while the walls are modeled using a system of doublets. A purely symmetric single degree of freedom pendulum motion did not amplify in the presence of walls. The addition of out-of-phase forcing in a second degree of freedom, however, amplified or damped the motion. The roll motion diverged in the presence of a simulated out of phase yaw motion. A subharmonic yaw oscillation superposed on the pendulum motion also amplified, and the amplification grew due to the proximity of walls. The results were correlated with observations from wind tunnel experiments of a scaled CONEX container. The results are used to develop metrics for wall effects in dynamic wind tunnel testing. The results show that such low-order simulation can be used to explore the development of instability due to interaction between different degrees of freedom.

NOTATION

$\mathbf{a_p}$	Acceleration vector of point P
A_{ref}	Surface area of box parallel to wind tunnel walls
C_p	Coefficient of Pressure
F	Forcing function
g	Acceleration due to gravity
I_{xx}	Moment of Inertia for load along X-X axis
I^P_{xx}	Moment of Inertia for load at point P along X-X axis
l	Tether length
M_P	Moment balance at point P
m_T	Total mass of body
n	Scaling factor
q_∞	Dynamic pressure
r	Radial coordinate measured from doublet position
$\mathbf{r_{pc}}$	Displacement vector of P from center of mass C
t	Simulation time
U_∞	Freestream velocity
V_θ	Orthogonal component of pendulum velocity
V_R	Radial component of pendulum velocity
Y	Modeled yaw function
α_p	Angular Displacement of the tethered load
θ	Polar angle measured from doublet position
κ	2D discrete doublet strength
ρ	Density of freestream

*Corresponding Author
Presented at the AHS 69th Annual Forum,Phoenix, Arizona, May 21–23, 2013.

INTRODUCTION

The proximity of walls can cause errors in wind tunnel testing. The usual rule of thumb in testing a static model in a low speed wind tunnel is to ensure that the blockage imposed by the model is no more than 5 percent of the cross-sectional area of the test section (Ref. 1). When the model moves inside the tunnel, dynamic wall effects are possible, and some guidance is needed to determine the permissible range of parameters for such experiments. The work in this paper was motivated by an observation made while investigating the behavior of a rectangular box suspended by tethers inside a wind tunnel. A scaled model of a CONEX container suspended using a single-point tether attachment to simulate a load slung from a helicopter, was tested in two different wind tunnels, a 1.07m x 1.07 m tunnel, and a 2.54m x 2.74 m John J. Harper

wind tunnel (see Figure 1). In the larger tunnel, the model was steady and stable at low speeds, while in the smaller tunnel the model started rotating at a low tunnel speed along with large-amplitude lateral pendulum swing and torsion, resulting in divergent oscillations. As the test time increased, the oscillations became large enough that the model hit the side walls of the tunnel. Prior work elsewhere had suggested that the behavior observed in the smaller tunnel agreed with flight observations of full scale CONEX container behavior (Ref. 2); however, this was in the presence of the swirl and downwash of a rotor wake in addition to the freestream.

The difference in the behaviors was suspected to be due to tunnel wall effects even though the blockage due to the model in the smaller tunnel was within standard acceptable limits ($\leq 5\%$ of cross sectional area). A full dynamic simulation from first principles using computational fluid dynamics would be an expensive undertaking as discussed in (Ref. 3). Instead, this motivated a study to generate a reduced-order simulation model in order to develop better metrics for tunnel sizing and possibly wall effect correction in dynamic unsteady wind tunnel testing. Similar phenomena may be expected in several other applications such as maneuvering vehicles, air-drop testing, and aerodynamic decelerator studies.

Oscillations of a slung load are considered to be divergent if the amplification rate or oscillation amplitude is above a certain threshold. Mechanisms that could initiate divergence include:

1. Yaw oscillations induced by:
   (a) Lateral motions (rolling) of the body
   (b) Unsteady flow experienced by the body
   (c) Phenomena which cause an asymmetric C_p distribution
2. Yaw oscillations can also couple with pitch through the action of drag forces that create fore-aft swing.
3. Yaw and lateral swing induced by vortex shedding.
4. Pitch-yaw coupling due to periodic drag oscillations driven by vortex shedding.

Wind tunnel wall effects have been extensively studied, and a comprehensive review is presented in (Ref. 1). Elementary fluid mechanics can be used to model these effects with sufficient accuracy. The doublet and vortex elements have been used in the past to model the effect of wind tunnel walls for steady test conditions (Refs. 4, 5). Wall interference effects on unsteady experiments has been studied primarily for oscillating wings and are presented in (Refs. 1, 6). However, there is limited knowledge on how proximal walls influence the fluid-structure interaction of tethered bluff bodies.

The objective of the work is thus to develop reduced-order models of aerodynamic tunnel wall interference suitable for incorporation into more sophisticated dynamic simulations for sling load aeromechanics, precision airdrop, rotorcraft handling qualities, and other eventual applications. These models are based on potential flow techniques that identify how proximal walls affect unsteady bluff body fluid-structure interaction. Presently the focus is on studying fundamental mechanisms that lead to the amplification of instability.

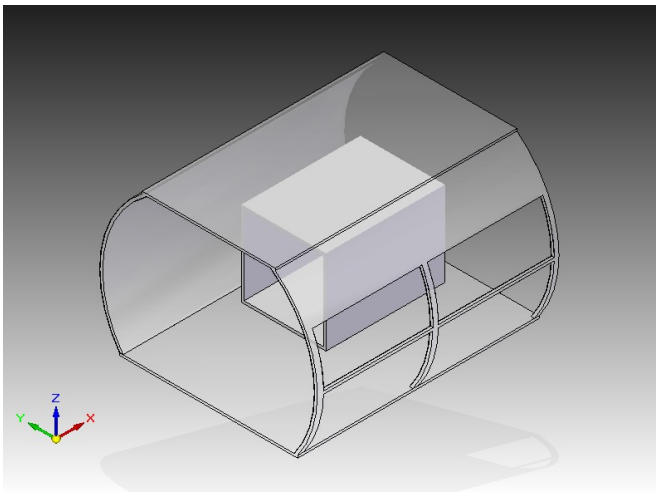

Fig. 1. Comparison of the 1.07m x 1.07m tunnel and the 2.13m x 2.54m tunnel.

METHODOLOGY

A demonstration sequence was developed using the *MATLAB*® and *Simulink*® software packages to systematically investigate the role of different degrees of freedom in amplifying the oscillations of a model in a wind tunnel. The body was assumed to be rigid. The body in the simulation is not hinged at its center of mass but at a point above it. The tether was assumed to consist of only a single rigid wire running from the top of the box to the gimbaled mount at the wind tunnel ceiling instead of the four metallic wires hooked on to the corners of the box in the actual wind tunnel experiments. The body could then be represented as a compound pendulum, shown in Figure 2.

From conservation of the angular momentum of a rigid body in two dimensional motion,

$$I_{xx}\ddot{\alpha}_P = \sum M_P - \mathbf{r_{pc}} \times m_T \mathbf{a_p} \tag{1}$$

Assuming the pivot point to be at Point P, Equation 1 simplifies to:

$$I^P_{xx}\ddot{\alpha}_P = \sum M_P \tag{2}$$

$$I^P_{xx}\ddot{\alpha}_P = -mglsin(\alpha_P) \tag{3}$$

The effects of the wall were simulated using a system of doublets (see figure 3(a) for illustration of a single doublet) representing elementary solutions to the Laplace equation describing mass conservation in terms of a velocity potential. The doublets were positioned using the method of images.

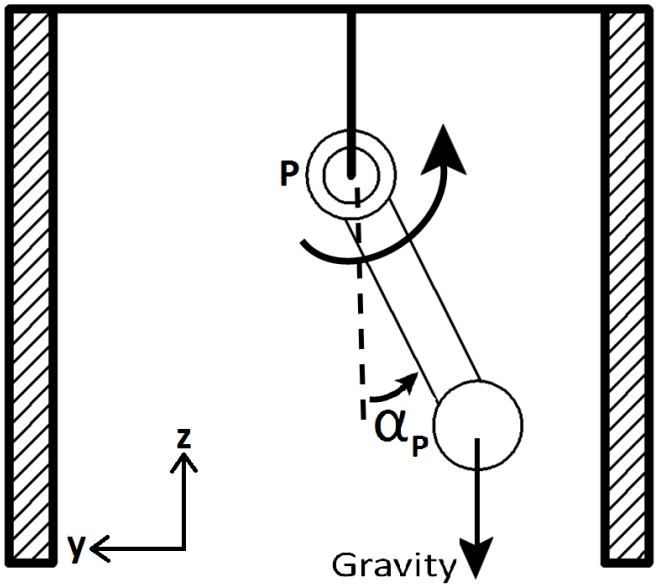

Fig. 2. Frontal view of the compound pendulum model inside the wind tunnel.

With the primary doublet positioned on the body, two other doublets were positioned as the primary's images behind the walls (illustrated in Figure 3(b)).

The velocity field around a doublet may be written in terms of the radial and azimuthal components at any given point, respectively as follows:

$$V_R = \left(U_\infty - \frac{\kappa}{r^2} \right) \cos(\theta) \tag{4}$$

$$V_\theta = \left(-U_\infty - \frac{\kappa}{r^2} \right) \sin(\theta) \tag{5}$$

The velocity of the pendulum motion is very small compared to the freestream velocity. Six different velocity values (two for each doublet) are resolved for the two faces of the box facing the wind tunnel walls. Then the dynamic pressure ($q_\infty = \frac{1}{2}\rho U_\infty^2$) is calculated at these two faces. Under the assumption of isentropic flow, stagnation pressure is then used in conjunction with dynamic pressure to calculate the static pressure at the two faces. Finally, using a reference area for the faces, a resultant suction force due to the induced velocity is calculated. This suction force is then used as a forcing function in the differential equation governing the motion of a compound pendulum:

$$I_{xx}^P \ddot{\alpha}_P = -mgl sin(\alpha_P) + l \cdot F \tag{6}$$

SEQUENCE OF SIMULATION EXPERIMENTS

Case 1: Pendulum motion in a freestream The first case simulates the harmonic pendulum motion using just a single doublet in the freestream. This doublet is located at the current position of the body in the freestream. Model parameters

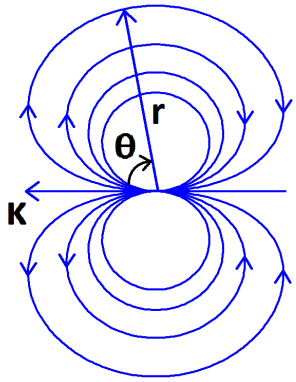

(a) A discrete 2D doublet with strength κ

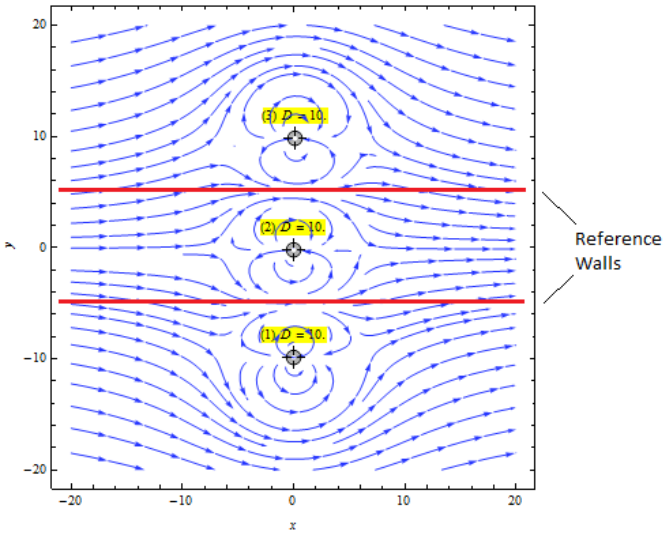

(b) Method of images (doublet in freestream)

Fig. 3. Illustration of doublets used in method of images

such as the body mass, sling length, and moment of inertia were selected to correspond to those of the model used in the wind tunnel experiments to maintain consistency. The body was subject to an initial displacement condition of $\alpha_P = 30°$. Expectedly, the result shows harmonic motion from $-30°$ to $+30°$. To verify the simulation parameters used in the model, the natural frequency of the tethered model was measured using experiments in still air. It was determined to be 3.737 rad/s. The natural frequency computed using the simulation in still air resulted in 3.767 rad/s, which is 0.8% different from the experimental value. The theoretical natural frequency in still air was calculated to 3.7667 rad/s which is also in agreement with the natural frequency calculated from the simulation.

Case 2: Addition of Tunnel walls In the second step of the sequence, two more doublets were added using the method of images to simulate the walls. Their location was determined at each step of the simulation as they have to correctly main-

tain the $\vec{V} \cdot \vec{n} = 0$ boundary conditions at the wall. Again, an initial condition of $\alpha_P = 30^\circ$ was used that also resulted in a simple harmonic motion with an amplitude of 30°. The wall force amplitude was also a harmonic function that was equal in magnitude and opposite in direction at the two extreme positions of the pendulum motion. These effectively cancelled out, so that there was no net amplification of the pendulum motion.

Case 3: Addition of an Out-of-phase force, with no walls As part of the third case in this sequence, the forcing function in the governing equation (Equation 6) was selected to be a signal that was out of phase of the pendulum motion. The two doublets added in Case 2 were removed to isolate the effect of an out of phase forcing function on the model in the freestream. The out of phase signal represented a yaw oscillation. A Fast Fourier Transform (FFT) was performed on the results of Case 1 to obtain the frequency used in the forcing function. It was added into the model so that:

$$F(t) = 0.056 \cdot sin(3.76 \cdot t + \pi/2) \tag{7}$$

The amplitude of this force relative to that of the primary wall effect force has a critical effect on the stability of the pendulum motion. Assuming a side force coefficient of π per radian, this force can be generated by yawing 1 degree. In other words, this is the force generated from a yaw oscillation of $\pm 1^\circ$ at a free stream of 8.94 m/s (speed at which divergence was observed in the smaller tunnel). Amplitudes greater than 0.056 resulted in divergence of the roll amplitude within 50 seconds. A more appropriate range of amplitudes must await further investigation by correlation with quasi-steady load data from the wind tunnel and computational fluid dynamic simulations. The amplifying response of the model can be seen in Figure 4. The addition of an out-of-phase force at the same frequency as the primary pendulum motion can result in amplification and eventually in divergence of the motion.

Case 4: Addition of an out of phase force with walls In the fourth step of the sequence, the walls were added to the simulation of Case 3. The resulting motion of the pendulum is shown in Figure 5, and it can be seen that it is again an amplifying response. In comparison to Case 3, the amplification rate in Case 4 is higher (Figure 6). Note that the difference between the two cases was the addition of the tunnel wall forces.

Case 5: Subharmonic yaw forcing In the fifth step of this demonstration sequence, the model was still subject to two degrees of freedom (roll and yaw oscillations). However, the yaw oscillations were externally added into the system after observing the results of the wind tunnel experiments in the smaller tunnel. Yaw oscillations were seen to occur at approximately half the frequency of the roll oscillations. Hence, the following signal was used as the yaw oscillation signal:

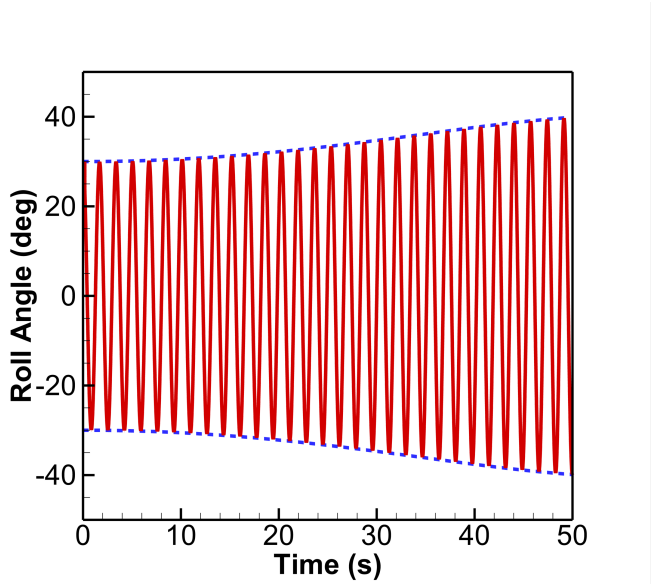

Fig. 4. Amplification of the pendulum motion coupled with an out-of-phase force in a freestream, in the absence of walls.

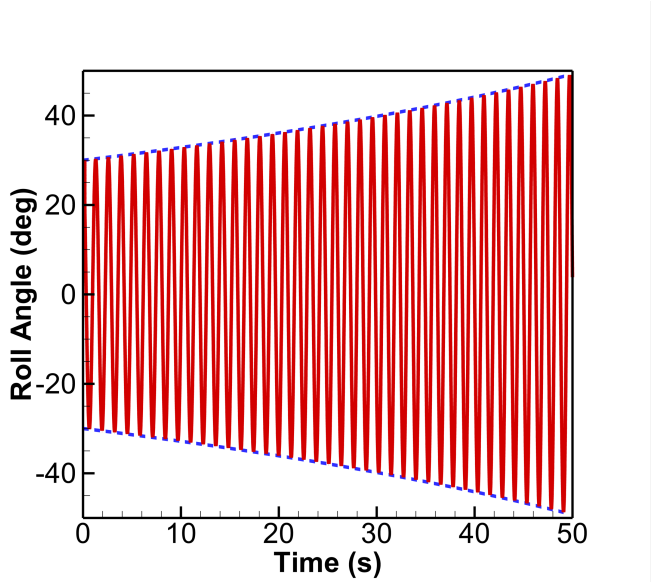

Fig. 5. Amplification of the pendulum motion coupled with out-of-phase force in a freestream, in presence of walls.

$$Y(t) = 0.143 \cdot sin\left(\frac{3.76}{2} \cdot t + \frac{\pi}{2}\right) \tag{8}$$

The simulation applied this yaw attitude signal to generate a force based on a side force coefficient slope of π per radian, where the force magnitude changed direction depending on whether the yaw attitude is positive or negative. Positive yaw attitude was along the positive z-axis. Positive yaw attitude produced a force in the negative y-axis and vice versa. As can seen in Figure 7, amplification was observed in the pendulum motion. The Forcing function used in this demonstration sequence was found to be of the same order as those expected

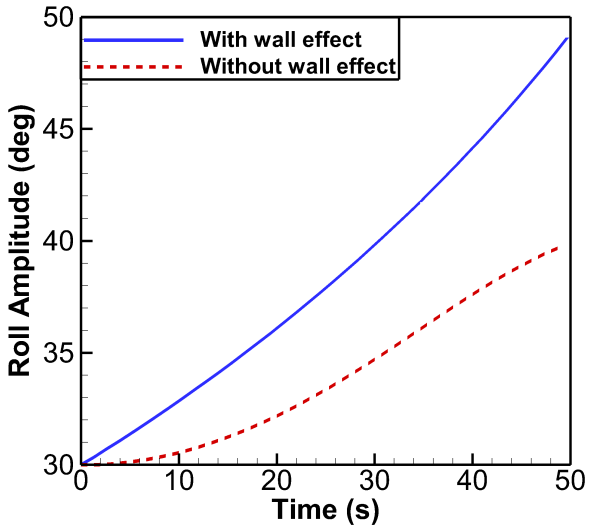

Fig. 6. Amplification rates of Case 3 (no walls) and Case 4 (walls present).

from the side forces seen in CFD simulations of the CONEX container in (Ref. 3)

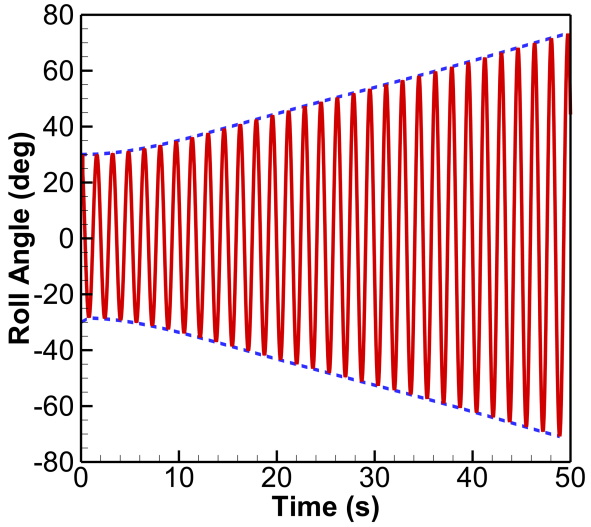

Fig. 7. Amplification rates of Case 3 (no walls) and Case 4 (walls present).

Case 6: Wind Tunnel Dynamic Wall Effect Metric Case 5 was repeated for varying wind tunnel test section widths and box widths to capture the change in amplification, as measured by the peak amplitude of oscillation at 25 seconds. Each simulation began starting with the same 30-degree initial condition in each run. Then two other cases were run to identify a relation between the flatness of the bluff body (relative amount of flat side that it has to cause the suction effects that contribute to wall effects) and the wall effect on amplification. Flatness of the body is thus defined for this purpose as:

$$flatness = \frac{A_{ref}}{PlanformArea} = \frac{A_{ref}}{Length \cdot Depth} \tag{9}$$

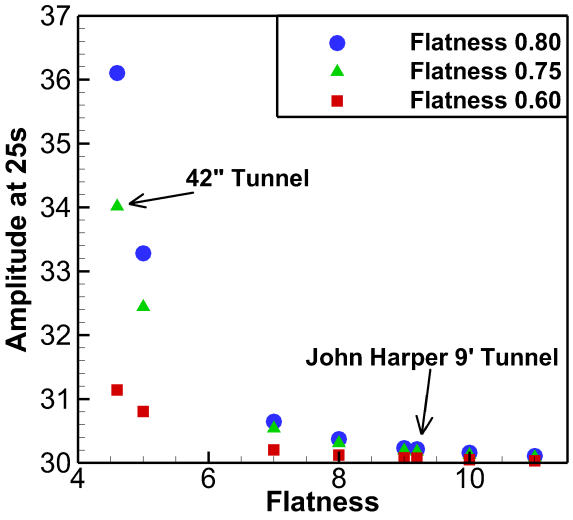

Fig. 8. Dependence of amplification on flatness of test model.

Hence, a thin flat plate placed normal to the flow, the traditional metric for blockage, flatness will approach zero whereas for a finite width box the flatness ≥ 1. From Figure. 8 it can be seen that at time t = 25 seconds, the amplitude of pendulum motion is higher in the case of the 1.07m x 1.07m wind tunnel as compared to the John J. Harper Wind Tunnel facility (test section width of 2.74m or 9 feet).

COMPARISON TO EXPERIMENTAL DATA

Video analysis of the wind tunnel videos for the CONEX was done to determine the validity of the coefficients used in the forcing function of the Simulink model. It was noted that in the case of the larger John Harper Wind Tunnel there was transition from the narrow side facing the airflow to broad side facing the airflow; this occurs during the speed range of 15.6-17.9 m/s. For the 1.07m x 1.07m wind tunnel this event occurs at 6.7m/s. However there is spinning behavior starting at 4.5 m/s. By averaging the frequencies of oscillation at different speeds in the video footage of the 1.07m x 1.07m wind tunnel, the frequency of the roll oscillations was computed as 3.702 radians per second. After computing the results of Case 5 with variables (such as moment of inertia of the load, sling length, distance from the walls etc.) used in experimentation in the 1.07m x 1.07m wind tunnel, the frequency of roll oscillation was calculated to be 3.8948 radians per second. This frequency is approximately 5% greater than the roll frequency

observed in the experiment and suggests that there is coupling between yaw oscillations with roll oscillations leading to a divergent behavior. The video analysis of the wind tunnel experiment reaffirms this as the CONEX container performs steady yaw oscillations in conjunction with lateral swinging at 13.4 m/s.

CONCLUSIONS

In this paper, a sequence of simple mathematical simulations is used to illustrate how to simulate the basic mechanisms by which a tethered rectangular may develop divergent oscillations in the presence of a proximal wall. In summary,

1. The flow between the rectangular body and the tunnel walls produces a suction which in turn produces a force on the rectanular body. With only one degree of freedom, a pendulum motion, this suction is symmetric and does not contribute to instability.
2. With two degrees of freedom, namely a lateral swing and a forcing function that is out of phase with the lateral swing, the body experiences divergence.
3. The amplification rate is substantially increased with wall proximity.
4. A subharmonic yaw oscillation appears to be a mechanism that is present in wind tunnel experiments. This is shown to cause amplification for the simulations.
5. This paper shows that a reduced fidelity simulation with multiple degrees of freedom can provide guidance on the mechanisms of instability and divergence in the behavior of slung loads in a freestream.
6. For dynamic testing, the quasi-steady blockage criterion is insufficient to ensure that wall effects are negligible.

This simulation can thus provide guidance on the effects of proximal walls in amplifying the oscillations due to fluid-structure interaction of a tethered bluff body. Although motivated by the case of unsteady wall effect, a potential flow simulation framework at this level of complexity shows promise to provide physical insight into tethered bluff body instability mechanisms and the role of interaction between degrees of freedom. Complex pressure distributions and tether dynamics could be systematically introduced into the simulation to study instability mechanisms.

ACKNOWLEDGMENTS

This work is part of Task 10 of the Vertical Lift Rotorcraft Center of Excellence project at Georgia Tech, funded by the US Army and NASA. The technical monitor is Dr. Michael Rutkowski.

We acknowledge the assistance of Sorin Pirau of the Experimental Aerodynamics Group with the measurements and computation aspects related to this project. Authors also acknowledge valuable discussions with Daniel Prosser in the Computational Aeroelasticity lab.

REFERENCES

[1]Garner, H. C., Rogers, E., Acum, W., and Maskell, E., "Subsonic wind tunnel wall corrections," Technical report, DTIC Document, 1966.

[2]Raz, R., Rosen, A., Carmeli, A., Lusardi, J., Cicolani, L., and Robinson, D., "Wind Tunnel and Flight Evaluation of Passive Stabilization of a Cargo Container Slung Load," *Journal of the American Helicopter Society*, Vol. 55, (3), 2010, pp. 032001.

[3]Prosser, D. and Smith, M., "Navier-Stokes-Based Dynamic Simulations of Sling Loads," AIAA Structures, Structural Dynamics, and Materials Conference, Boston, MA, May April 8–11, 2013, 2013.

[4]Rizk, M. and Smithmeyer, M., "Wind-tunnel wall interference corrections for three-dimensional flows," *Journal of Aircraft*, Vol. 19, (6), 1982, pp. 465–472.

[5]Mokry, M., Digney, J., and Poole, R., "Doublet-panel method for half-model wind-tunnel corrections," *Journal of Aircraft*, Vol. 24, (5), 1987, pp. 322–327.

[6]Vos, R., "Wall Correction Methods for Dynamic Tests," Technical report, NATO Science and Technology Organization, 1998.